Atomic Force Microscopy of Polymer Crystals. 6. Molecular Imaging and Study of Polymorphism in Poly(*p*-phenyleneterephthalamide) Fibers

D. Snétivy and G. J. Vancso*

Department of Chemistry, University of Toronto, 80 St. George Street, Toronto, Ontario M5S 1A1, Canada

G. C. Rutledge

Department of Chemical Engineering, Massachusetts Institute of Technology, Cambridge, Massachusetts 02139

Received July 13, 1992

ABSTRACT: The macromolecules in extended-chain crystals of as-spun and annealed poly(*p*-phenyleneterephthalamide) fibers and the microfibrillar morphology were visualized by atomic force microscopy (AFM). Quantitative information about the crystal lattice on the surface of the fibrils was obtained. The positions of the phenylene groups with respect to the hydrogen-bonded sheet of the crystal lattice were visualized. Results are compared with structures deduced from X-ray diffraction measurements on one hand, and from predictions for polymorphic forms of the crystal structure calculated in computer simulation experiments on the other. Periodicities and registration angle obtained for annealed fibers are consistent with reported crystal modifications. Analyses of images captured on as-spun fibers indicate the existence of a new polymorphic form (modification III) which was suggested by computer simulations but has not been previously observed experimentally. The AFM image of this new structure is consistent with successive phenylene rings along the chain being rotated in similar, rather than opposite, directions about the chain axes.

Introduction

Fibers spun of rigid macromolecules from lyotropic solutions of poly(*p*-phenyleneterephthalamide) (PPTA) contain highly oriented chains in their extended conformation and are well-known for their ultrahigh modulus and strength and good thermal stability.[1] Commercially available PPTA fibers, registered under the trademark Kevlar, are grouped into a few categories which have different combinations of properties associated with structural variations that result from different forming (i.e. spinning) conditions.[2] On the basis of wide-angle X-ray diffraction (WAXD) data a model was proposed[3] for the crystal structure of annealed PPTA fibers. The suggested unit cell is monoclinic (pseudoorthorombic) with the cell parametes $a = 7.87$ Å, $b = 5.18$ Å, c (chain direction) = 12.9 Å, and $\gamma \approx 90°$. This crystal structure was subsequently confirmed and designated modification I.[4] In addition, later WAXD studies unveiled that upon coagulation of PPTA with water another stable structure can also exist (modification II),[4] which is a variation of modification I with unit cell parameters $a = 8.0$ Å, $b = 5.1$ Å, c (chain direction) = 12.9 Å, and $\gamma \approx 90°$. In this modification the chain conformation is maintained, with location of the second chain in the unit cell shifted from $[1/2,1/2]$ to $[1/2,0]$ in the ab facet. Such polymorphic behavior is a very common phenomenon in crystalline polymers and is due to the nearly isoenergetic packing of macromolecules with identical conformation.[5]

The characterization, understanding, and control of the formation of different polymorphic forms of polymers, and naturally of Kevlar, is essential for materials design since various modifications can differ significantly in physical properties. Also, volume changes associated with solid-state transitions from one polymorphic form to another can result in undesirable dimensional instability of the end-use products. WAXD has been the most frequently used technique to characterize the crystal structure of various polymorphic forms of semicrystalline polymers.[5] It yields composite information, integrated over the scattering volume of the sample, about unit cell parameters, chain-packing, and chain conformation. Imperfections in crystal structure and the possible coexistence of polymorphic forms result in broadened and overlapping lines in the WAXD pattern, often making structural determination difficult or impossible. For example, as-spun PPTA fibers prior to annealing showed broad overlapping WAXD maxima, and the diffraction lines were resolved only after heat treatment.[6] The annealing protocol used to improve X-ray pattern resolution does so presumably at the expense of less stable structural variants present in the as-spun fibers, thus precluding the study of these other polymorphs by WAXD.

A detailed atomistic simulation of oriented PPTA suggested the importance of structural motifs in determining polymer packing geometry. On this basis, as many as six polymorphic forms, in addition to those two previously observed by WAXD, were identified as having nearly identical multichain packing energies.[7] The existence of one or more of these or related structures which might occur e.g. as the as-spun, nonannealed fibers, has not yet been confirmed by X-ray analysis, presumably due to the aforementioned experimental difficulties.

With the advent of atomic force microscopy (AFM) a novel technique has become available which can be used to visualize atoms and molecules at the surface of polymeric materials, as well as to study morphology on the micrometer scale.[8,9] The use of AFM has been reported to study macromolecular chains in extruded polyethylene,[10] characteristics of polymer lamellar crystals on the micrometer scale,[11,12] and macromolecules in extended-chain crystals of poly(oxymethylene) (POM)[13] and polypropylene[14] and to visualize different crystal planes on the surface of oriented ultrahigh molecular-weight polyethylene,[15] to mention but a few examples. In addition, selective visualization of oxygen atoms and methylene groups in POM was also achieved.[13]

The AFM probes the sample surface with a very sharp tip (ideally terminated by a single atom or a few atoms

0024-9297/92/2225-7037$03.00/0

only) attached to a microfabricated cantilever which contacts the surface by a low force, typically of the order of 10^{-7} to 10^{-10} N. (For a technical review see ref 16). An optical lever technique, for example, can be used to detect the deflection of the microcantilever. The sample is mounted on a piezo tube which controls the relative position of the scanned surface with respect to the tip. The interatomic forces between the apex of the tip and atoms in the surface are a function of the tip position with respect to the surface and reflect the arrangement of atoms at the sample surface. The composite force results in the deflection of the cantilever, the detection of which is converted to an optical image by a computer workstation.

In a short preliminary paper[17] we have already reported on molecular imaging of PPTA by AFM. In this paper we present a detailed AFM study of PPTA molecules as as-spun and annealed fibers.

Experimental Section

PPTA fibers (Kevlar, DuPont) were resolubilized in 100% H_2SO_4 and dry-jet wet-spun through a 1-cm air gap into an aqueous coagulation bath and subsequently collected on a wind-up roller rotating at a velocity sufficient to ensure a low (approximately 1:1 spinerette velocity:wind-up velocity) draw ratio. Of the samples discussed in this work, the larger diameter fiber was spun at 80 °C and 20 m/min from a 17.5% by weight polymer-in-acid solution into a 7 °C bath using a 200-μm-diameter monofilament spinerette; the smaller diameter fiber was spun at 30 °C and 40 m/min from a 10% by weight solution into a 25 °C bath using a 54-μm-diameter monofilament spinerette. The latter fiber sample was then twice annealed in an argon atmosphere at 450 °C for a total of 40 s. On the basis of previous studies, annealing is expected to result in recrystallization processes in the fiber which promote larger crystallites and predominance of the thermodynamically most stable crystal structure, with accompanying increase in elastic modulus and tenacity.[18,19] Further details of the spinning process are described elsewhere.[6]

AFM imaging was performed on the larger diameter, as-spun fibers as well as the smaller diameter annealed fiber. The corresponding diameters for these fibers, as determined by laser diffraction,[20] were 103 ● 2 μm and 23.0 ± 0.5 μm for the as-spun and annealed fibers, respectively. Because of their larger diameters, variation in coagulation rate with radial position and lack of postspin annealing, the as-spun fibers are expected to exhibit greater cross-sectional heterogeneity and lower average degree of molecular orientation, manifested in a skin–core structure as well as possible spatial variation in crystal morphology. These larger diameter fibers are especially useful as AFM specimens due to the resulting ease of preparation of the samples for microscopy (see below). However, the poor resolution of WAXD patterns made crystal structure determinations in these fibers impractical. Typical equatorial scans for as-spun and annealed fibers (obtained by using a Siemens D-500 X-ray diffractometer equipped with a bent-quartz monochromator and a scintillation counter) are illustrated in Figure 1. Further analysis of the annealed materials by WAXD confirms their crystal structure to be largely that of modification I.

AFM images were taken in air using a NanoScope II instrument (Digital Instruments) with D- and A-type scan heads (the latter was used for molecular resolutions) utilizing NanoProbe 100-μm triangular Si_3N_4 microcantileves with thick legs; the effective spring constant as specified by the supplier was 0.58 N m^{-1}. In the terminology of Digital Instruments, imaging was usually performed in the "height mode"; however, some images were captured in the "force mode". ("Height mode" means that the force between the AFM tip and the sample surface is held constant by the electronic feedback loop. The vertical displacement of the tip, which is needed to maintain the chosen force, is then recorded as the tip is scanned over the sample surface.) On AFM images differences in the gray tones correspond to variations in the measured displacement. Raw data of images with molecular resolution were obtained with the low-pass filter set to 1 and the high-pass filter to 4; however, for some of the images with

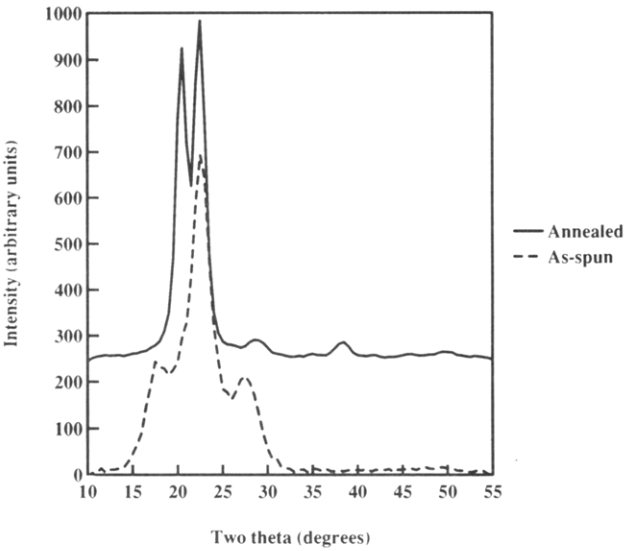

Figure 1. Equatorial traces of the WAXD fiber pattern typical of as-spun (- - -) and annealed (—) PPTA fibers.

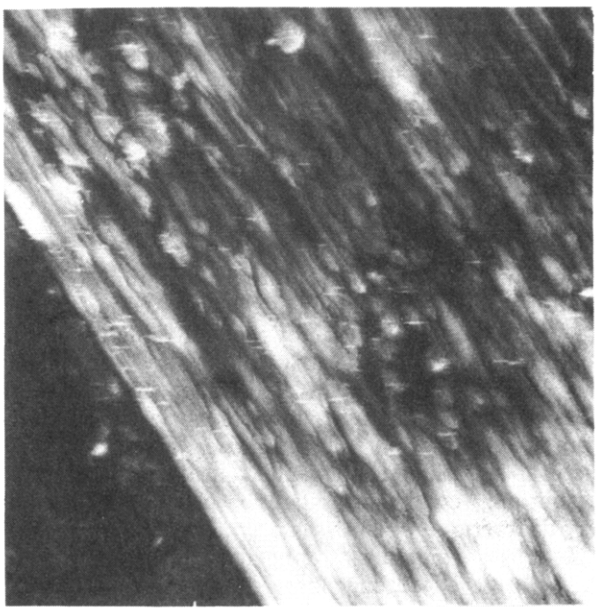

Figure 2. AFM micrograph (image size: 15 μm × 15 μm) of a cleaved annealed PPTA fiber embedded in epoxy resin.

molecular resolution and for all of the images on the micrometer scan size all filters were disengaged. The images were very stable and reproducible. Electrostatic charges sometimes caused problems, especially after sample cleaving; in such cases good images were obtained after a 24-h waiting period. Graphite and mica images with angstrom resolution were used for distance calibration of the lateral position of the piezo controller.

Prior to AFM imaging, the PPTA fibers were embedded in epoxy resin (Araldit Standard, Ciba-Geigy) and cleaved in the fiber direction using a Sorval MT6000 ultramicrotome with glass knives. An AFM image of the cleaved surface of the annealed fiber (scan size: 15 μm × 15 μm) is shown in Figure 2. The microtomed surface of the epoxy can be seen clearly in the left-bottom corner of the photomicrograph. The rest of the image shows the expected microfibrillar morphology.[21] Microfibrils which were cut through during microtoming can also be observed; for example, seven fibrils surrounding a black spot at ca. one-third height from the bottom and two-thirds from the left edge of the photomicrograph can clearly be spotted.

Results and Discussion

A. Images of Annealed Fibers. A typical photomicrograph showing a 1-μm × 1-μm scan area of PPTA

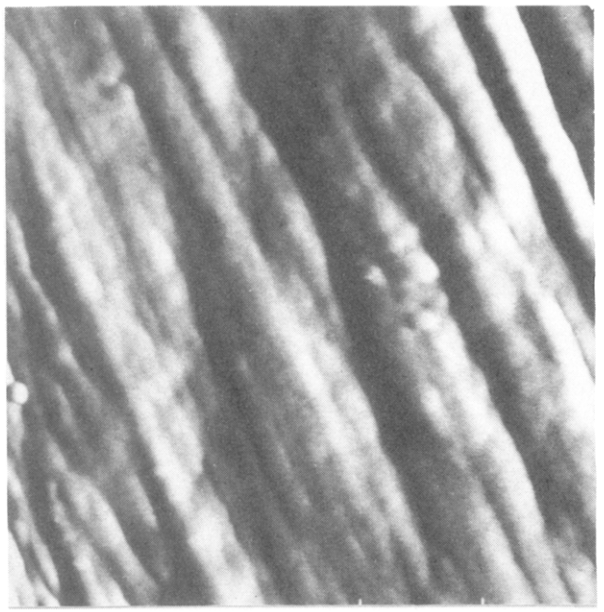

Figure 3. AFM micrograph (image size: 1 μm × 1 μm) of the surface of an annealed PPTA fiber showing microfibrillar morphology.

microfibrils is shown in Figure 3. On the basis of surface profile analysis the microfibrils had an average diameter of 50 ± 20 nm. Images with molecular resolution were obtained on the surface of such microfibrils. A typical image (raw data; scanned area is 5 nm × 5 nm) exhibiting resolution of features on the molecular level in both the x (horizontal) and the y (vertical) directions is shown in Figure 4. During imaging the fiber sample axis lay at a known inclination of 25° counterclockwise from the y axis of the image. This information was necessary to assign details of the image to the PPTA molecule. Under the aforementioned spin conditions, PPTA crystallites exhibit angles of inclination generally within 15° of the fiber direction.[6,18] Knowing the fiber direction therefore enabled us to estimate the chain direction in the images. On the top and bottom margin of Figure 4 the two markers correspond to the expected chain direction. In this case the a priori information about molecular alignment was necessary to identify the polymer chains. However, in many cases, such as the example captured in Figure 5, the direction of macromolecular alignment is self-evident. Again, in Figure 5, the chain direction is labeled by the markers on the margins. It is worth mentioning that the microfibrillar axis showed some distribution about the axis of the fiber direction for both the as-spun and the annealed fibers, but the macromolecular direction and the axis of the microfibrils on which the molecular resolution was obtained agreed to within ±5° for all of the images.

Periodicities of the short-range order both perpendicular and along a line inclined with respect to the chain direction (denoted the axial and lateral periodicities, respectively) and the angle between these two directions (denoted the angle of registration; a value of 90° indicates neighboring chains in perfect axial register) were obtained by analyzing the two-dimensional autocorrelation pattern (2-D AP) of the nanographs. A typical example using an image of average quality (raw data) and the corresponding 2-D AP are shown in Figures 6 and 7, respectively. For these images the analysis of the 2-D AP resulted in an average axial periodicity C of 12.5 Å in the chain direction and a lateral periodicity B of 4.9 Å with a registration angle α_{BC} of 90°. These values agree well with the repeat distance

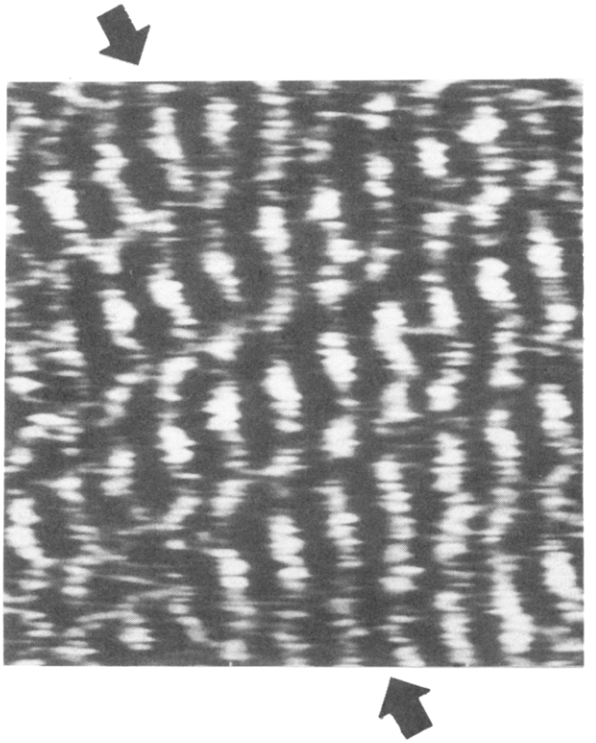

Figure 4. AFM nanograph (image size: 5 nm × 5 nm) of an annealed PPTA microfibril with molecular resolution. The expected chain direction is shown by the arrows on the margin.

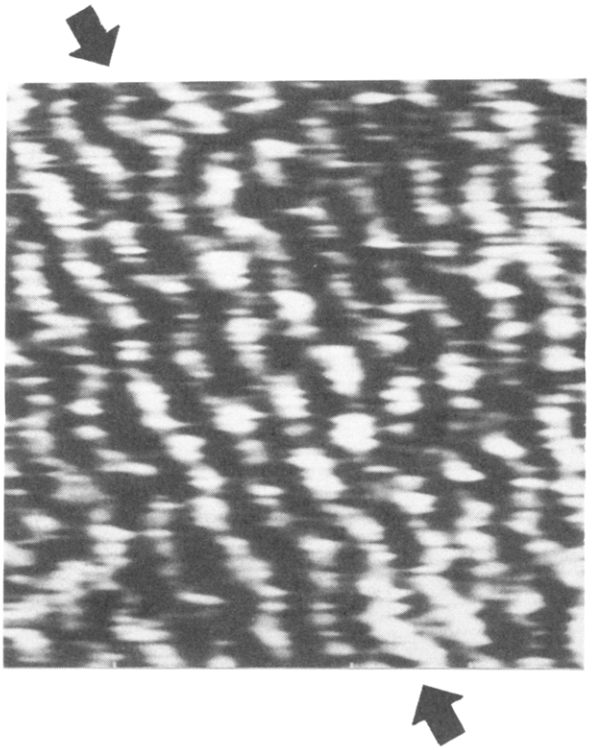

Figure 5. AFM nanograph (image size: 5 nm × 5 nm) of an annealed PPTA microfibril with molecular resolution. The chain direction, indicated by the arrows, is clearly visible.

(12.9 Å) in the crystallographic c (or chain) direction of the PPTA crystal structure (modification I), the crystallographic b repeat length (5.18 Å), and the angle α (=90°). Thus, details of the imaged area shown in Figures 6 and 7 are consistent with the parameters of the bc facet (the hydrogen-bonded sheet) of modification I. An analysis of ca. 50 images with molecular resolution obtained on annealed fibers was consistent with the parameters of this

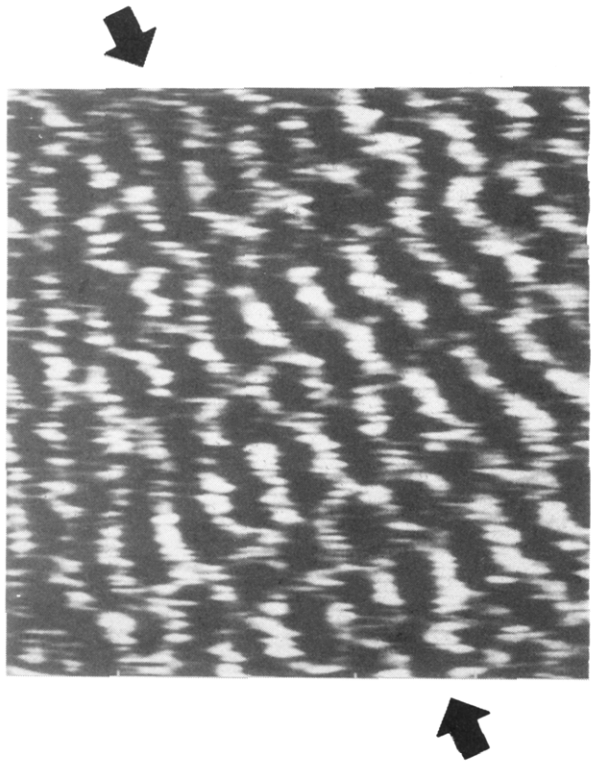

Figure 6. Typical AFM nanograph (image size: 5 nm × 5 nm) of an annealed PPTA microfibril of modification I (or II) with molecular resolution.

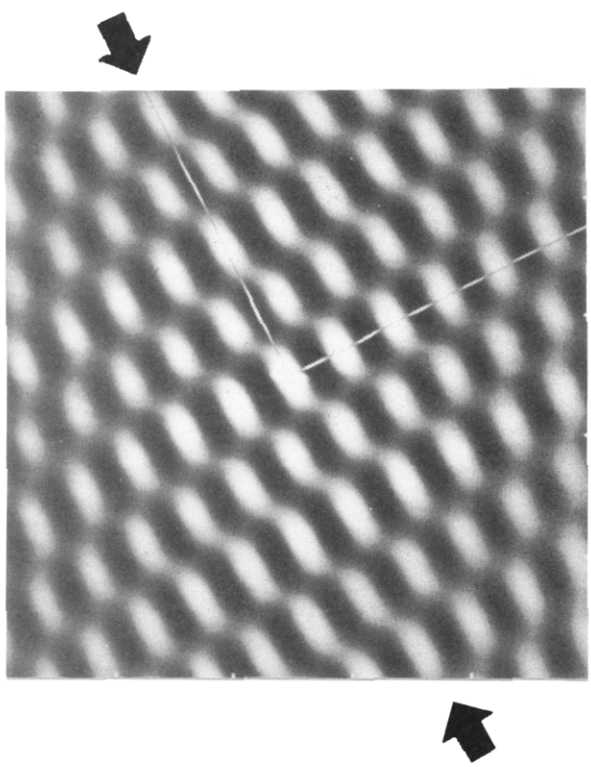

Figure 7. Two-dimensional autocorrelation pattern of the image shown in Figure 6. The value of the registration angle α_{BC} is 89°.

crystal plane; i.e., in all of these cases the *bc* facet was imaged. This is in accord with the expectation that, upon microtoming, the cleave surface of the crystals would occur predominantely in plane with the hydrogen-bonded sheets due to the relatively weak intermolecular forces (compared to the in-plane hydrogen-bonding forces) acting between sheets. It should be mentioned that molecular resolution was obtained only in discrete spots on the sample surface

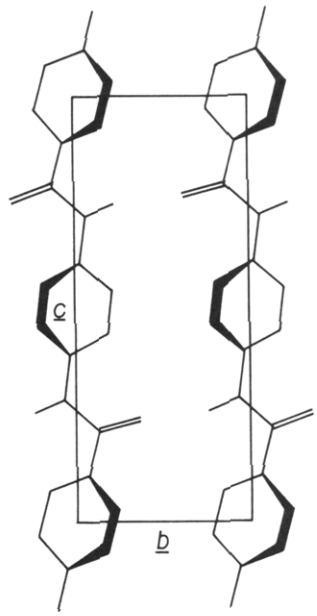

Figure 8. The *bc* of the crystal unit cell of modification I of PPTA (projection of the unit cell viewed from the crystallographic *a* direction).

over areas of ca. 6–10 nm × 6–10 nm. The error in the packing parameters obtained from AFM and the close similarity between *bc* crystallographic facets in modifications I and II do not allow us to distinguish between these two forms in our results.

Results of both X-ray studies and atomistic simulations have shown that successive phenylene rings along the chain are rotated in opposite directions by 30–40° out-of-plane with the amide linkage[3,7] in both modification I and II. A diagram of the *bc* facet of this crystal unit cell, depicting the skeletal structure of two chains (projection viewed from the crystallographic *a* direction), is shown in Figure 8. The bold lines illustrate the edges of the benzene rings which are above the *bc* plane of the projection in the true three-dimensional structure, corresponding to the alternating tilt angles mentioned above. In an AFM scan the tip deflection in the contact-mode imaging (which is dominated by repulsive interatomic forces) of this facet will be stronger if the atom(s) at the apex of the tip is(are) above the "protruding" edges of the aromatic rings. Figure 9 shows a typical image after Fourier reconstruction (noise filtering) and an overlay plot of the molecular structure on the same scale. Bright areas on this AFM image are consistent with higher contact forces resulting from the interaction of the tip with the alternating edges of the aromatic groups in the PPTA chains. In addition, hydrogen bonds perpendicular to the backbone direction resulted in a relatively high contact force between tip and sample and can be spotted clearly in the image. The observation of the alternating orientation of the phenylene groups with respect to the plane of the hydrogen-bonded sheet demonstrates the possible use of AFM to study macromolecular conformation in the solid state.

B. Images of As-Spun Fibers. A typical AFM image of microfibrils of the as-spun fiber (obtained in the constant-force mode) is shown in Figure 10. Analysis of 2-D AP of a series of nanographs with molecular resolution yielded packing parameters typical for modification I and fully consistent with the foregoing analysis of annealed fibers. In addition, we also recorded repeatedly images of microstructures which were inconsistent with either modification I or II, obtained e.g. from a point such as that with coordinates (870.0 nm, 743.5 nm). (In this notation

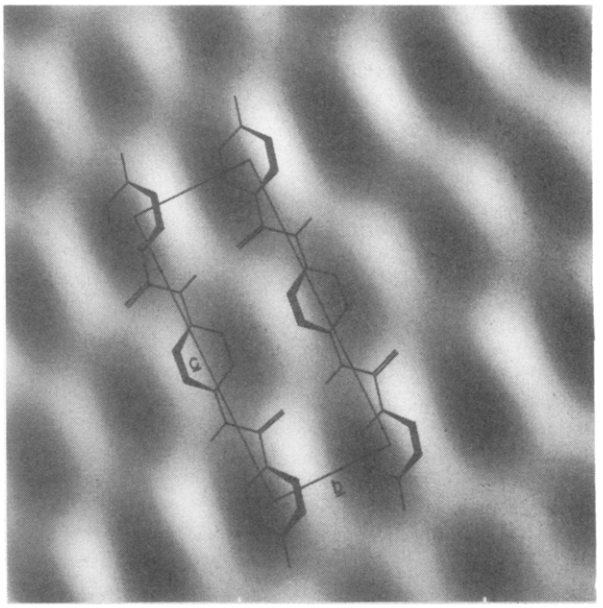

Figure 9. Fourier reconstruction of a typical AFM image of annealed PPTA; the overlay plot shows the corresponding facet of the unit cell.

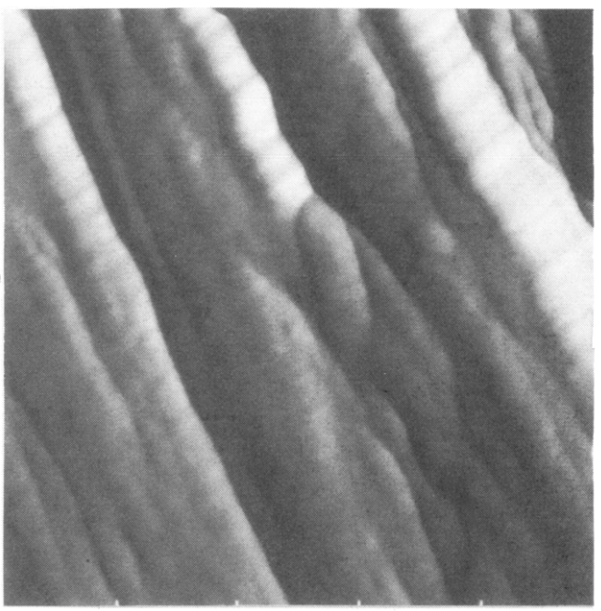

Figure 10. AFM micrograph (image size: 1 μm × 1 μm) of the surface of an as-spun PPTA fiber.

the first coordinate is the horizontal, and the second is the vertical distance from (0,0), where (0,0) corresponds to the left-bottom corner of the image.) The corresponding nanograph with molecular resolution is captured in Figure 11. It is worth mentioning that this image was obtained without using *any* filters; i.e. data were taken directly from the scan head in the "force imaging mode" using the cantilever deflection signal. The 2-D AP of the nanograph of Figure 11 is shown in Figure 12; again, the markers refer to the chain direction. A quantitative analysis showed that the registration angle for the depicted structure is 77° (see the overlay lines on the 2-D AP) which differs significantly from the 90° angle of modifications I and II. (The estimated accuracy in registration angles is 2°). Images with similar characteristics were obtained from other areas of the as-spun polymer with registration angles consistently close to 80°. In addition, the lateral periodicity was slightly smaller than that observed for modification I (or II). We tentatively denote this new structure

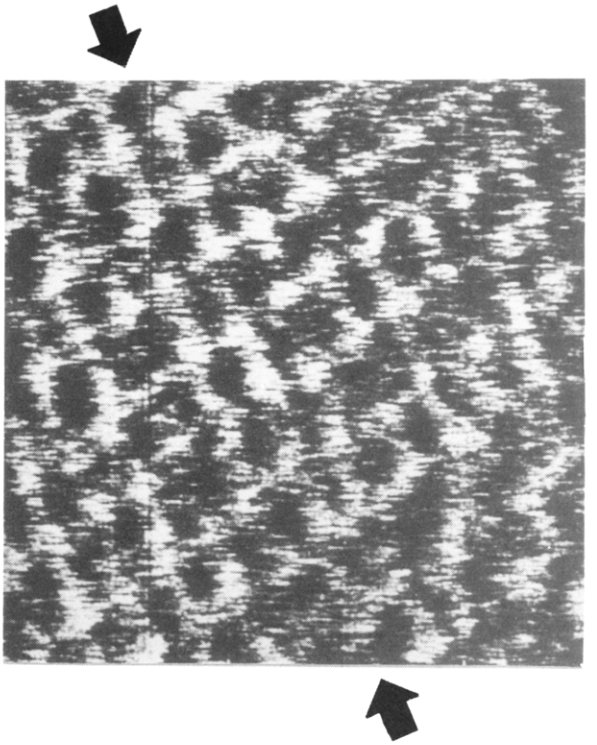

Figure 11. AFM nanograph (image size: 5 nm × 5 nm) of an as-spun PPTA microfibril (modification III). The expected chain direction is shown by the arrows on the margin. All filters were disengaged during capturing of this image.

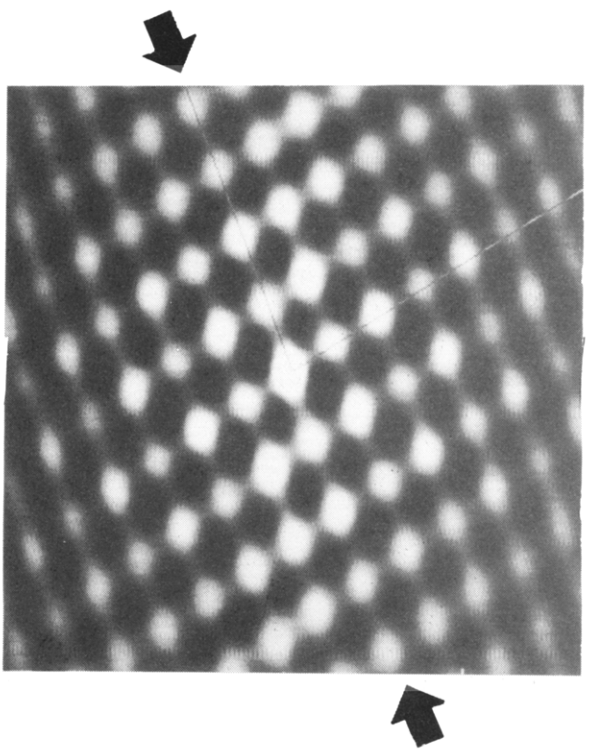

Figure 12. Two-dimensional autocorrelation pattern of the image shown in Figure 11. The value of the registration angle α_{BC} is 77°.

as modification III. Table I summarizes the observed periodicities and registration angles obtained in AFM experiments for this and the previous microstructures; the values are based on results obtained from 20 scans for the annealed sample and 7 scans for each modification of the as-spun fiber. The packing characteristics of modification III are similar to those reported as structure 6

Table I
Structural Parameters of PPTA Fibers from AFM[a]

	B (Å)	C (Å)	α_{BC} (deg)
as-spun, modification I or II	5.1 ± 0.2	12.7 ± 0.4	91 ± 2
annealed, modification I or II	4.8 ± 0.2	12.7 ± 0.7	88 ± 2
as-spun, modification III	4.5 ± 0.2	12.8 ± 0.6	80 ± 2

[a] C = chain periodicity; B = lateral periodicity; α_{BC} = registration angle.

from the computer simulations of ref 7; the calculated values from that work are b = 4.6 Å, c = 13.1 Å, and α = 79°.

In contrast to the images from both annealed and as-spun fiber indexed on the *bc* facet of modification I (or II), the AFM images of modification III do not exhibit the features characteristic of opposite rotation of successive phenylene rings along the chain (Figure 9). While there remains some discrepancy in the *shapes* of features observed in Figures 11 and 12, the location of bright spots in line with the chain axis is consistent with nearly coplanar aromatic rings (i.e. like rotation of successive phenylene rings). Such conformations are also characteristic of structure 6 anticipated by computer simulation. The like rotation of rings is likely to incur only a modest penalty in intramolecular conformational energy; this is readily offset by intermolecular packing forces. While it is not possible by AFM to verify the full three-dimensional geometry of structure 6 (modification III), the agreement between simulation and experiment for the *bc* facet is very good. To our knowledge, this is the first instance of experimental confirmation of a new polymorphic form subsequent to its prediction by computer simulation.

AFM thus allows, by means of selective imaging of spatially disparate regions of a sample, the resolution of multiple coexisting microstructures in polymorphous samples. While AFM does not currently share the same level of precision or three-dimensional structural information content as obtainable by WAXD, it does allow unique insight into atomic scale arrangements and degree of structural variation within a sample, information which is notoriously difficult to decipher by conventional polymer WAXD techniques.

Acknowledgment. Financial support by the Ontario Centre for Materials Research is gratefully acknowledged. The authors wish to thank the DuPont Chemical Co. for the donation of the sample material, Mr. B. Glomm for his help with the preparation of the samples, and the Swiss Federal Institute of Technology (ETH-Zürich) for the use of the fiber spinner and the X-ray diffractometer.

References and Notes

(1) Jaffe, M. In *Encyclopedia of Polymer Science and Engineering*; Kroschwitz, J. I., Ed.; Wiley: New York, 1987; Vol. 7, p 698.
(2) Dhingra, A. K. In *Encyclopedia of Polymer Science and Engineering*; Kroschwitz, J. I., Ed.; Wiley: New York, 1987; Vol. 6, p 756.
(3) Northolt, M. G. *Eur. Polym. J.* **1974**, *10*, 799.
(4) Haraguchi, K.; Kajiyama, T.; Takayanagi, M. *J. Appl. Polym. Sci.* **1979**, *23*, 915.
(5) Corradini, P.; Guerra, G. *Adv. Polym. Sci.* **1992**, *100*, 183.
(6) Rutledge, G. C.; Suter, U. W.; Papaspyrides, C. D. *Macromolecules* **1991**, *24*, 1934.
(7) Rutledge, G. C.; Suter, U. W. *Macromolecules* **1991**, *24*, 1921.
(8) Binnig, G.; Rohrer, H. *Rev. Mod. Phys.* **1987**, *59*, 615.
(9) Marti, O.; Ribi, H. O.; Drake, B.; Albrecht, T. R.; Quate, C. F.; Hansma, P. K. *Science* **1988**, *239*, 50.
(10) Magonov, S. N.; K. Quarnstrom, K.; V. Elings, V.; Cantow, H.-J. *Polym. Bull.* **1991**, *25*, 689.
(11) Patil, R.; Kim. S. J.; Smith, E.; Reneker, D.; Weisenhorn, A. L. *Polym. Commun.* **1990**, *31*, 455.
(12) Snétivy, D.; Vancso, G. J. *Polymer* **1992**, *33*, 432.
(13) Snétivy, D.; Vancso, G. J. *Macromolecules* **1992**, *25*, 3320.
(14) Snétivy, D.; Guillet, J. E.; Vancso, G. J. *Polymer*, in press.
(15) Snétivy, D.; Yang, H.; Vancso, G. J. *J. Mater. Chem.* **1992**, *2*, 891.
(16) Sarid, D. *Scanning Force Microscopy With Applications to Electric, Magnetic, and Atomic Forces*; Oxford University Press: Oxford, U.K. 1991.
(17) Snétivy, D.; Rutledge, G. C.; Vancso, G. J. *Polym. Prepr. (Am. Chem. Soc., Div. Polym. Chem.)* **1992**, *33*, 786.
(18) Magat, E. E. *Philos. Trans. R. Soc. London, Ser. A* **1980**, *294*, 463.
(19) Dhingra, A. K. In *Encyclopedia of Polymer Science and Engineering*; Kroschwitz, J. I., Ed.; Wiley: New York, 1987; Vol. 6, p 756.
(20) Perry, A. J.; Ineichen, B.; Eliasson, B. *J. Mater. Sci. Lett.* **1974**, *9*, 1376.
(21) Panar, M.; Avakian, P.; Blume, R. C.; Gardner, K. H.; Gierke, T. D.; Yang, H. H. *J. Polym. Sci., Polym. Phys. Ed.* **1983**, *21*, 1955.

Registry No. PPTA (copolymer), 25035-37-4; PPTA (SRU), 24938-64-5.